John Caffey Award. Sonography of the Caudal Spine and Back: Congenital Anomalies in Children

Thomas P. Naidich, Sandra K. Fernbach, David G. McLone and Arnold Shkolnik

AJNR Am J Neuroradiol 1984, 5 (3) 221-234
http://www.ajnr.org/content/5/3/221

John Caffey Award

Sonography of the Caudal Spine and Back: Congenital Anomalies in Children

Thomas P. Naidich[1]
Sandra K. Fernbach[1]
David G. McLone[2]
Arnold Shkolnik[1]

Articulated-arm, B-mode 3.5–5.0 MHz sonograms from 27 children with congenital anomalies of the caudal spine were analyzed *retrospectively* and correlated directly with patient appearance, preoperative myelograms, intraoperative photographs, and pathologic specimens to determine how effectively sonography could display the major pathologic features known to be present. Anterior spina bifida, posterior spina bifida, and (partial) sacral agenesis were displayed as focal absence of normal spinal echoes and distortions of the paraspinal/gluteal muscles. Subcutaneous anechoic spaces continuous with the spinal canal through a spina bifida identified the presence, site, and configuration of each meningocele present. Highly echoic masses were easily discerned at the sites of 14 of 16 lipomas and at the solid fibroadipose portions of both sacrococcygeal teratomas. Echoes from the surface of the spinal cord and occasionally from the central canal identified abnormally low cord position in 16 of 17 cases and identified herniation of the cord (or filum) into a concurrent meningocele in seven of 10 cases. Sonographic display of an anechoic meningocele bordered by a lobular, highly echoic, subcutaneous lipoma that inserted onto a low-lying or herniated spinal cord reliably identified lipomyelomeningocele. Despite limitations discussed in the text, initial experience suggests that sonography will be a useful method for screening patients for possible tethered spinal cord, (lipo)(myelo)meningocele, sacrococcygeal teratoma, and other anomalies of the caudal spinal axis.

In patients with myelodysplasia and other anomalies of the caudal spine, cranial sonography has been widely accepted for assessing concurrent intracranial pathology and for intraoperative placement of ventricular shunt catheters [1–3]. Renal sonography has proved equally valuable for detecting associated renal agenesis, renal ectopia, and hydronephrosis [4, 5]. Spinal sonography, however, has received relatively little attention, even though sonographic windows are provided by the incomplete ossification of the posterior elements in children under 1 year of age and by spina bifida [6–19].

Initial reports of spinal sonography performed with automated scanners [8] and with real-time equipment [9, 15, 17] have suggested that sonography could be useful for displaying the structural deformities of congenital spinal anomalies. Preliminary results with articulated-arm, B-mode sonography have confirmed its utility in caudal spinal anomalies [10]. We present the results of a retrospective study undertaken for two reasons: (1) to discern the precise nature of the structures imaged sonographically and (2) to explore more fully the potential of sonography for displaying congenital anomalies of the caudal spine.

Materials and Methods

Preoperative B-mode sonography was performed with a Rohnar 7000 scanner (North American Philips Co.) using 3.5 and 5.0 MHz transducers in 27 children with abnormalities of the caudal spine admitted to Children's Memorial Hospital, Chicago, from February 1980 through August 1983. In each patient, the lumbosacral spine, associated subcutaneous mass,

This article appears in the May/June 1984 issue of *AJNR* and the June 1984 issue of *AJR*.

Received September 26, 1983; accepted after revision January 23, 1984.

Presented in part at the Symposium Neuroradiologicum, Washington, DC, October 1982, and the annual meeting of the Society for Pediatric Radiology, Atlanta, April 1983.

[1] Department of Radiology, Children's Memorial Hospital and Northwestern University Medical School, 2300 Children's Plaza, Chicago, IL 60614. Address reprint requests to T. P. Naidich.

[2] Division of Neurosurgery, Children's Memorial Hospital and Northwestern University Medical School, Chicago, IL 60614.

***AJNR* 5:221–234, May/June 1984**
0195-6108/84/0503-0221 $00.00

TABLE 1: **Final Diagnoses in Children with Congenital Anomalies of the Caudal Spine and Back**

Final Pathologic Diagnosis	No. Patients
Lipoma of the filum terminale with tethering	1
Lipoma of the filum terminale with normal position of conus	1
Spinal lipoma or lipomyelomeningocele with tethering*	12
Spinal lipoma with tethering, distant simple meningocele and hydromyelia	1
Simple meningocele	1
Postoperative myelomeningocele with retethering	2
Cloacal extrophy with myelocystocele, tethering, and hydromyelia	1
Anterior sacral meningocele with partial sacral agenesis, tethering, and intramedullary sacral dermoid	1
Complete sacral agenesis†	2
Sacrococcygeal teratoma	2
Sacrococcygeal "malformative process," possibly teratoma	1
Isolated pilonidal sinus	1
Pilonidal sinus with partial sacral agenesis	1
Total	27

* Among these 12 cases, there was one instance each of cord fixation (tethering) in the high lumbar region so the conus still lay in normal position; partial sacral agenesis; and distant "unrelated" pilonidal sinus. In this group, extension of lipoma into the filum terminale was common and has not been enumerated specifically.

† One of the two had concurrent hydromyelia.

TABLE 2: **Efficacy of Sonography in Imaging Congenital Spinal Anomalies**

Anatomic Deformity	No. Patients Studied by Sonography		
	Totals	Positive	"Negative"
Abnormally low position of spinal cord	17	16	2
Extracanalicular extension of cord or filum	10	7	3
Hydromyelia	3	3	3
Meningocele (as at least one component of the lesion)	15	15	3
Lipoma	15	14	2
Wholly intracanalicular mass (sacral dermoid)	1	1	1
Sacral agenesis (partial or complete)	5	3	2
Sacrococcygeal teratoma or "malformative process"	3	3	1
Pilonidal sinus	3	3	0

Note.—*Positive* refers to the patients in whom sonography displayed the deformity; *negative* refers to the patients in whom the structures imaged by sonography likely could NOT be appreciated on prospective interpretation.

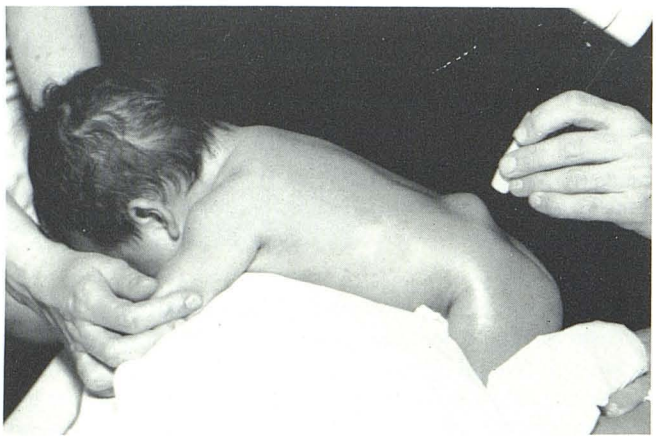

Fig. 1.—Patient position to distend caudal meningoceles for sonography. Throughout this article, all lateral and sagittal views are oriented with anterior to reader's left.

Fig. 2.—Normal anatomy and pilonidal sinus in 8-year-old boy. Midsagittal sonogram of sacral region demonstrates intense curvilinear echo of normal skin surface (*arrowheads*); smooth, hypoechoic normal subcutaneous tissue plane; and hyperechoic contour of normal sacrococcygeal spine. Pilonidal sinus (*arrow*) appears as abnormal midline, hyperechoic, triangular skin thickening, which in this patient extends deeply toward coccyx, but remains separated from coccyx by anechoic cleavage plane.

and buttocks (as necessary) were examined in the prone position with serial sonographic sections at 1, 2, or 5 mm intervals in the longitudinal (sagittal) plane and at 2, 5, or 10 mm intervals in the transverse (axial) plane. In selected cases, sections oblique to the sagittal plane were obtained to demonstrate continuity between paramedian meningoceles and the midline spinal canal. In each of the 27 cases, the preoperative sonograms were analyzed retrospectively by direct comparison with patient photographs, plain spine radiographs, water-soluble contrast myelography, and water-soluble contrast computed tomographic (CT) myelography. In all but the two patients with complete sacral agenesis, the sonograms were also correlated directly with surgical observation, intraoperative photographs, and pathologic specimens obtained.

The 27 patients were 1 day to 9 years old. Sixteen were under 1 year of age, including 10 who were 3 months of age or younger. Twelve were boys and 15 girls. Table 1 summarizes the final pathologic diagnoses in the 27 patients. Seventeen children had low position of the spinal cord, 15 had meningoceles, and 15 had lipomas.

Patient Position

Patients with caudal spinal anomalies are best positioned with the upper body elevated and the lower body flexed (fig. 1) for two reasons:

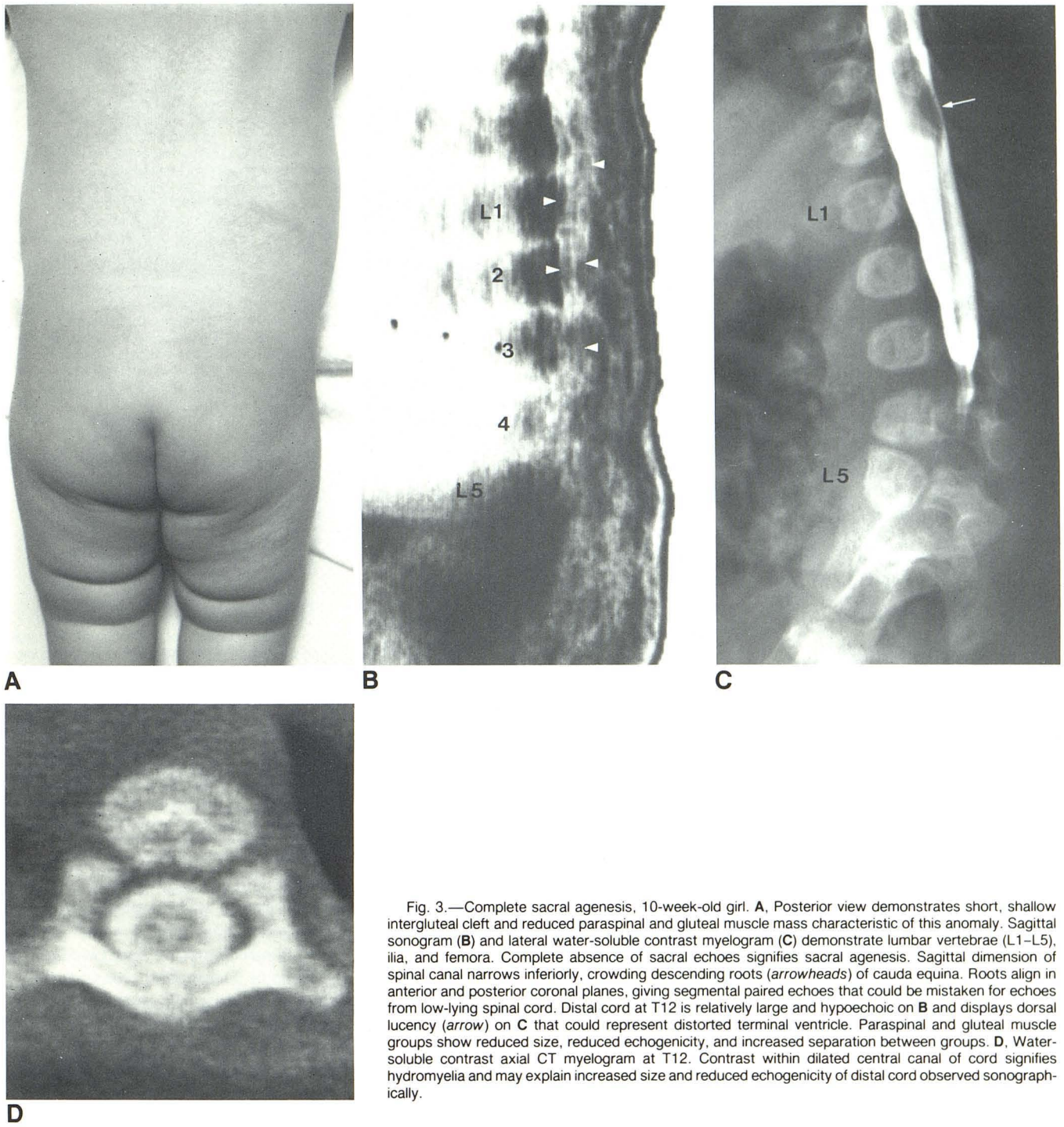

Fig. 3.—Complete sacral agenesis, 10-week-old girl. **A**, Posterior view demonstrates short, shallow intergluteal cleft and reduced paraspinal and gluteal muscle mass characteristic of this anomaly. Sagittal sonogram (**B**) and lateral water-soluble contrast myelogram (**C**) demonstrate lumbar vertebrae (L1–L5), ilia, and femora. Complete absence of sacral echoes signifies sacral agenesis. Sagittal dimension of spinal canal narrows inferiorly, crowding descending roots (*arrowheads*) of cauda equina. Roots align in anterior and posterior coronal planes, giving segmental paired echoes that could be mistaken for echoes from low-lying spinal cord. Distal cord at T12 is relatively large and hypoechoic on **B** and displays dorsal lucency (*arrow*) on **C** that could represent distorted terminal ventricle. Paraspinal and gluteal muscle groups show reduced size, reduced echogenicity, and increased separation between groups. **D**, Water-soluble contrast axial CT myelogram at T12. Contrast within dilated central canal of cord signifies hydromyelia and may explain increased size and reduced echogenicity of distal cord observed sonographically.

1. Hydrostatic pressure is greatest at the dependent end of a fluid column. The normal arachnoid sac, any hydromyelic cavity, and any meningocele are, therefore, distended maximally and best demonstrated sonographically in the dependent position. They are least distended and least well demonstrated when elevated above the spinal column. Cerebrospinal fluid (CSF) may even run out of a meningocele when the sac is raised above the spinal column, leading to temporary collapse of the sac (cf. fig. 5). Although patients with large anterior sacral meningoceles have been studied successfully in the supine position through the fluid-filled bladder [18, 19], small anterior sacral meningoceles are better detected in the head-elevated prone position. Patients with posterior meningoceles should be studied in the sitting or steeply inclined prone position with the head elevated far enough to overcome any tendency for the prone position

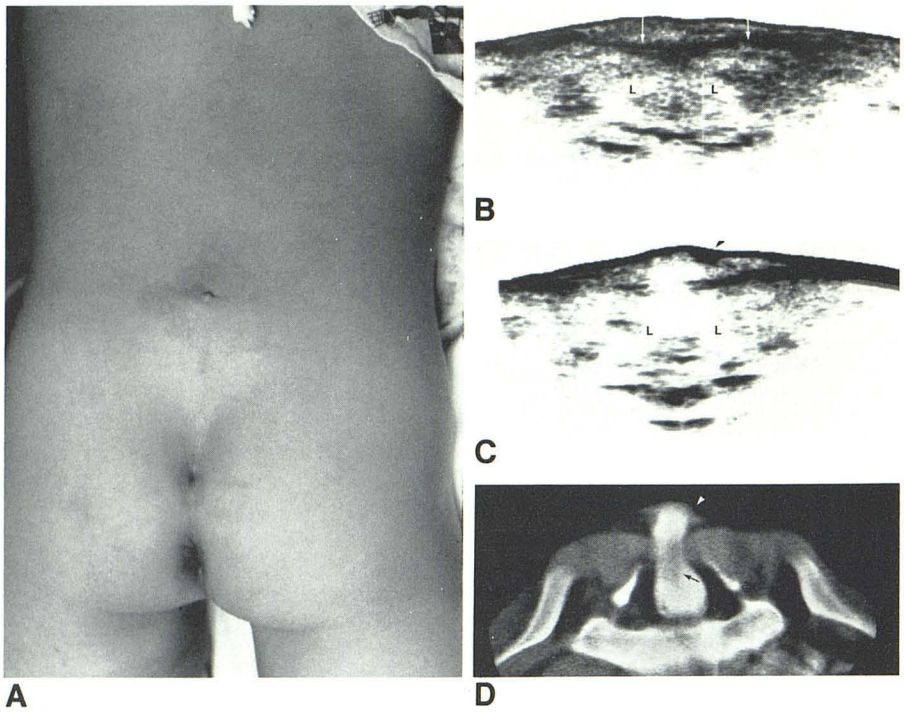

Fig. 4.—Spina bifida, 5-year-old boy with lipomyelomeningocele and sacrococcygeal dimple. **A**, Posterior view reveals skin-covered lumbosacral mass with skin tag and nevus situated above intergluteal cleft and separate, deep sacrococcygeal dimple. **B**, Transverse sonogram below spina bifida demonstrates intact skin cover, normal junction of posterior lumbodorsal fascia (*arrows*) at median raphe, symmetric echoic paraspinal muscles between fascia and subjacent anechoic laminae (L), and echoic contents of spinal canal. **C**, Transverse sonogram at spina bifida demonstrates midline deficiency in junction of posterior lumbodorsal fascia, separation of echoic paraspinal muscles, separation of anechoic laminae (L), and direct continuity of anechoic meningocele from spinal canal through midline fasciomuscular defect into subcutaneous space. Hyperechoic fat (*arrowhead*) indents dome of meningocele. Herniation of spinal cord was displayed on adjacent sections. **D**, Transverse water-soluble contrast CT myelogram at level comparable to **C** demonstrates same findings, including fat (*arrowhead*) indenting dome of meningocele. Herniating spinal cord (*arrow*) is well seen. (This case is also illustrated in [10].)

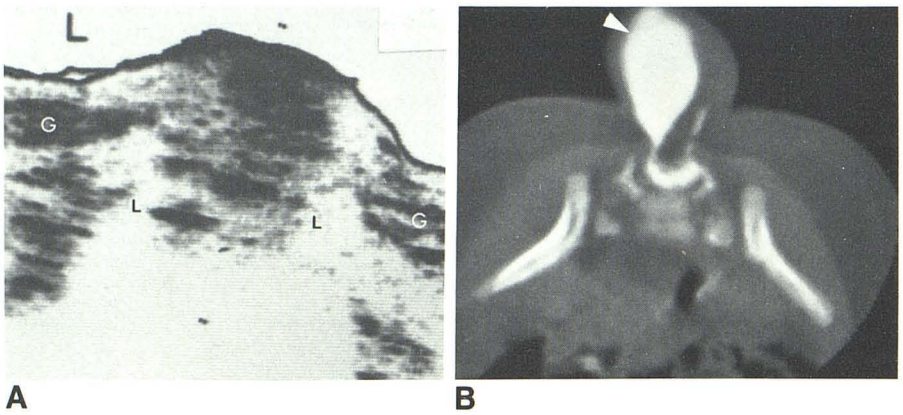

Fig. 5.—Spina bifida, transverse section, 1-month-old girl with lipomyelomeningocele. **A**, Transverse sonogram, prone with head lower than rump, demonstrates no meningocele per se. Disruption of anechoic subcutaneous tissue plane in midline, wide separation of echoic fascia and subjacent gluteal muscles (G), and wide separation of anechoic laminae (L) indicate direct continuity of hyperechoic lipoma from subcutaneous space through spina bifida into spinal canal. **B**, Axial water-soluble contrast CT myelogram at level comparable to **A** demonstrates excellent distension of meningocele (*arrowhead*) because CT was obtained in head-elevated supine position with patient elevated above table to avoid compression of sac. Relations of sacrum, sacral laminae, iliac wings, and gluteal and iliopsoas muscles are well displayed by both sonography and CT. (This case is also illustrated in [10].)

to collapse the posterior sac. It is inadvisable to scan patients with posterior spina bifida in the supine position [8] unless the lesion is elevated above the water bath or support table, because the patient's own weight may compress and collapse a meningocele and drive extracanalicular lipoma and herniated cord inward to "create" an intracanalicular pseudotumor.

2. The length of the "acoustic window" created by spina bifida is limited by the normal vertebrae above (and often below) the defect. The width of the acoustic window created by incomplete ossification of the posterior elements of the spine is limited by the adjacent ossified parts of the laminae, and therefore narrows progressively with age. These limitations can be minimized by flexing the child to widen the interlaminar spaces and by angling the transducer cephalically, as in performing a spinal tap, to slip the beam between the laminar plates (fig. 1). In our experience, sonography of the caudal spine is performed most successfully under certain conditions: (1) the child is draped around a large bolster that keeps the head elevated and still bends the lumbosacral spine into a kyphosis and (2) the transducer is angled cephalad. The older and more ossified the spine, the more critical is the proper patient flexion and the proper beam angulation.

Results

Many patients manifested multiple, concurrent anomalies. Table 2 presents the incidence of each specific anatomic deformity and retrospective analysis of the efficacy of sonographic imaging of that deformity. Systematic analysis of the sonograms for normal anatomy and for the corresponding pathology revealed the following.

Normal Skin and Subcutaneous Tissue. Pilonidal Sinuses

The normal skin surface appears as an intensely echogenic line (fig. 2). The normal subcutaneous tissue appears as a

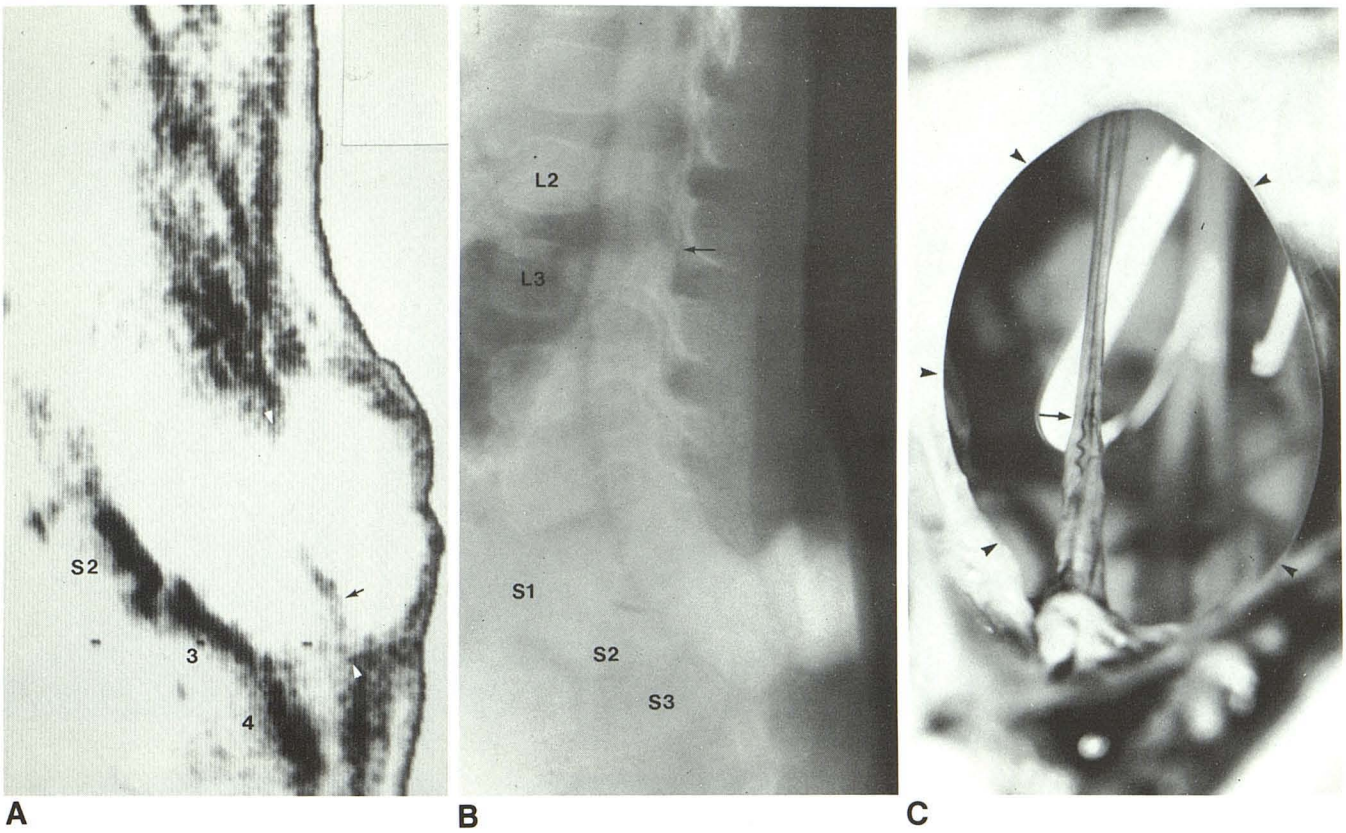

Fig. 6.—Simple meningocele, 1-year-old girl. **A**, Midsagittal sonogram demonstrates sacral vertebrae (S2–S4) and absence of posterior sacral elements at S1–S3, indicating focal sacral spina bifida. Lumbosacral mass is large anechoic meningocele directly continuous with enlarged spinal canal through relatively narrow hernia ostium (*arrowheads*). Thin wall of sac and absence of internal echoes signify this is a simple meningocele not associated with tethered cord. Filum terminale (*arrow*) passes to lower edge of hernia ostium. **B**, Lateral water-soluble contrast myelogram confirms sonographic findings. Spinal cord ends at L2–L3 (*arrow*). **C**, Posterior view of surgical field after midline incision collapsed meningocele. Ring of tissue (*arrowheads*) is ostium of meningocele. Filum terminale (*arrow*) inserts into lower edge of hernia ostium, as in **A**. Intense white highlights are reflections of ring-flash from CSF pooled within spinal canal. (Reprinted from [10].)

hypoechoic plane that is typically smooth and changes thickness gradually along the length of the image. This subcutaneous plane is better defined in older, more obese patients than in newborns or thin individuals.

In our series, sonography successfully displayed each of the three pilonidal sinuses as inward dimpling of the skin surface at the sinus ostium; markedly increased echogenicity and triangular thickening of the tissue along the sinus deep to the skin; and a clear, relatively anechoic separation between the deepest extent of the sinus and the normal spine beneath (fig. 2).

Normal Spinal Column and Paraspinal/Gluteal Muscles

The sonographic appearances of normal vertebrae seem to be distinctly different in the sagittal and transverse planes (figs. 3–7). On sagittal sonograms, normal vertebral bodies appear typically hyperechoic. Vertebral bodies seem to appear as hyperechoic "squares" or "bullet-shapes" that correspond to the full profiles of the bodies in lateral projection radiographs (fig. 3B). Vertebral bodies seem also to appear as hyperechoic lines or "smudges" that correspond to the posteriormost parts of the vertebral bodies (partial profiles) (fig. 3). In both cases, the posterior edges of these echoes mark the anterior wall of the spinal canal. Ossified laminae and spinous processes appear as hyperechoic lines or "smudges" that correspond to the anteriormost parts of the laminae and spinous processes. The anterior edges of these echoes mark the posterior wall of the spinal canal. Unossified laminae and spinous processes are not displayed.

In transverse sonograms (figs. 4 and 5), vertebrae seem to appear hypoechoic or anechoic, except for a few intense echoes from the anterior and posterior edges of the vertebral bodies. The vertebrae per se are thus difficult to appreciate but may be discerned by virtue of the surrounding paraspinal muscles (figs. 4 and 5).

Transverse sonography displays the normal paraspinal muscles as paired, symmetric, paramedian, inhomogeneously hyperechoic structures that converge medially to the median raphe (fig. 4B). These muscles are demarcated posteriorly by intense reflections from the superficial lumbodorsal fascia (fig. 4B). Transverse sonography displays the gluteal muscles as similar, paired, inhomogeneously hyperechoic structures situated posterior to the anechoic iliac bones (fig. 5B).

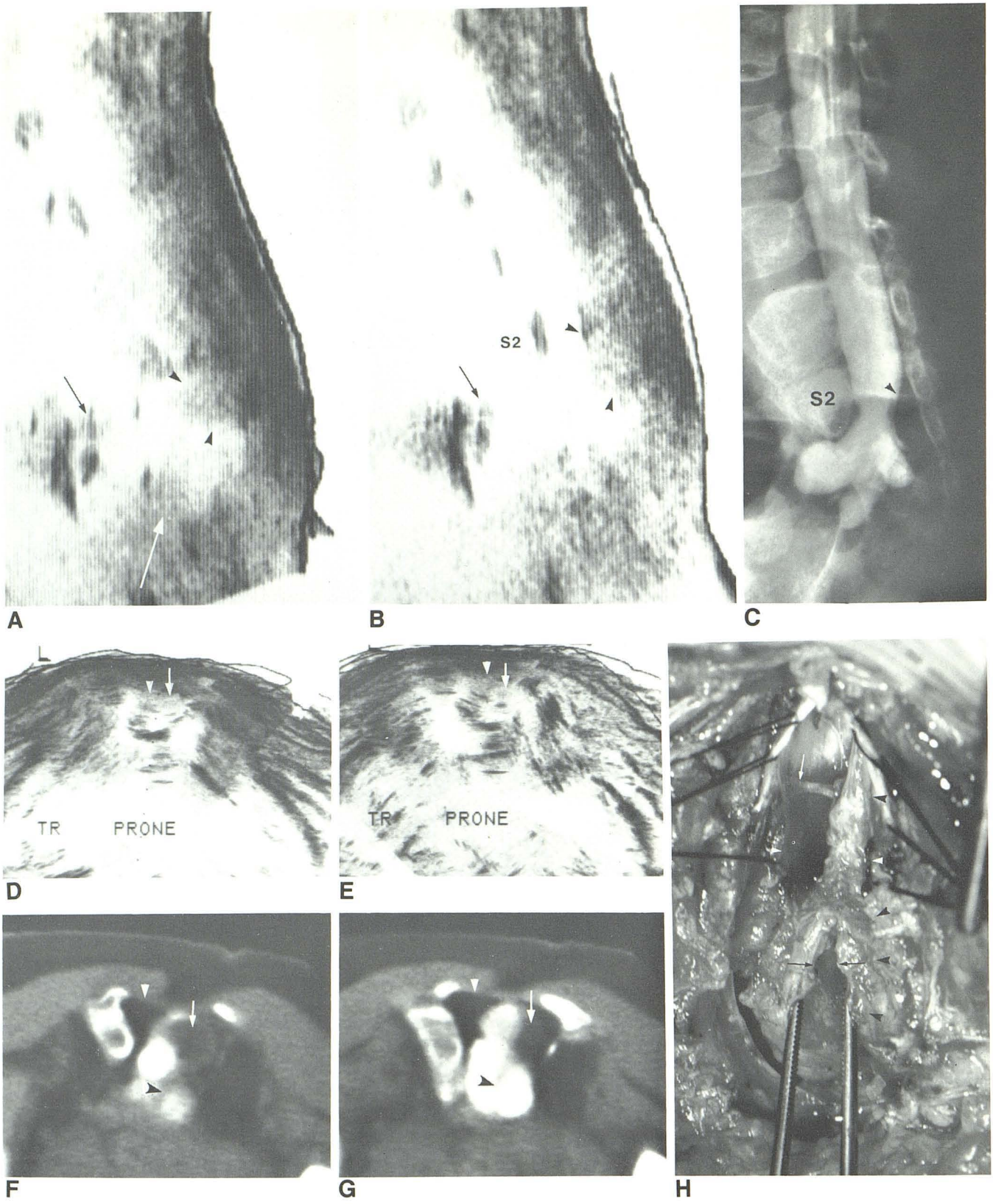

Fig. 7.—Anterior sacral meningocele with tethered cord and sacral intramedullary dermoid, 5½-year-old girl. Sagittal sonograms (**A** and **B**) and lateral water-soluble contrast myelogram (**C**). Focal absence of anterior and posterior sacral echoes indicates partial anterior and posterior sacral agenesis. Direct continuity of anechoic space from spinal canal through anterior sacral defect into pelvis and strong curvilinear echoes at anterior (deep) wall of space (*black arrows*) signify anterior sacral meningocele. Hyperechoic tissue (*arrowheads*) along posterior wall of sacral spinal canal corresponds to large extraarachnoid fat pad observed surgically. Round homogeneous echogenicity (*white arrow*) at lower end of spinal canal corresponds to wholly intracanalicular dermoid. Transverse sonograms (**D** and **E**) and axial water-soluble contrast CT myelograms (**F** and **G**) demonstrate larger left and smaller right part of bifid anechoic sacral vertebra, hyperechoic intracanalicular fat pad (*white arrowheads*), and mild, homogeneous echogenicity of sacral intramedullary dermoid (*arrows*). Extension of neural tissue (*black arrowheads*) to dome of anterior sac was not appreciated sonographically. **H**, Posterior view of surgical field demonstrates sacral subarachnoid space (*white arrowheads*), tethered spinal cord (*black arrowheads*) with laterally extending nerve root (*white arrow*), midline myelotomy (*black arrows*), and intramedullary dermoid (between tips of forceps).

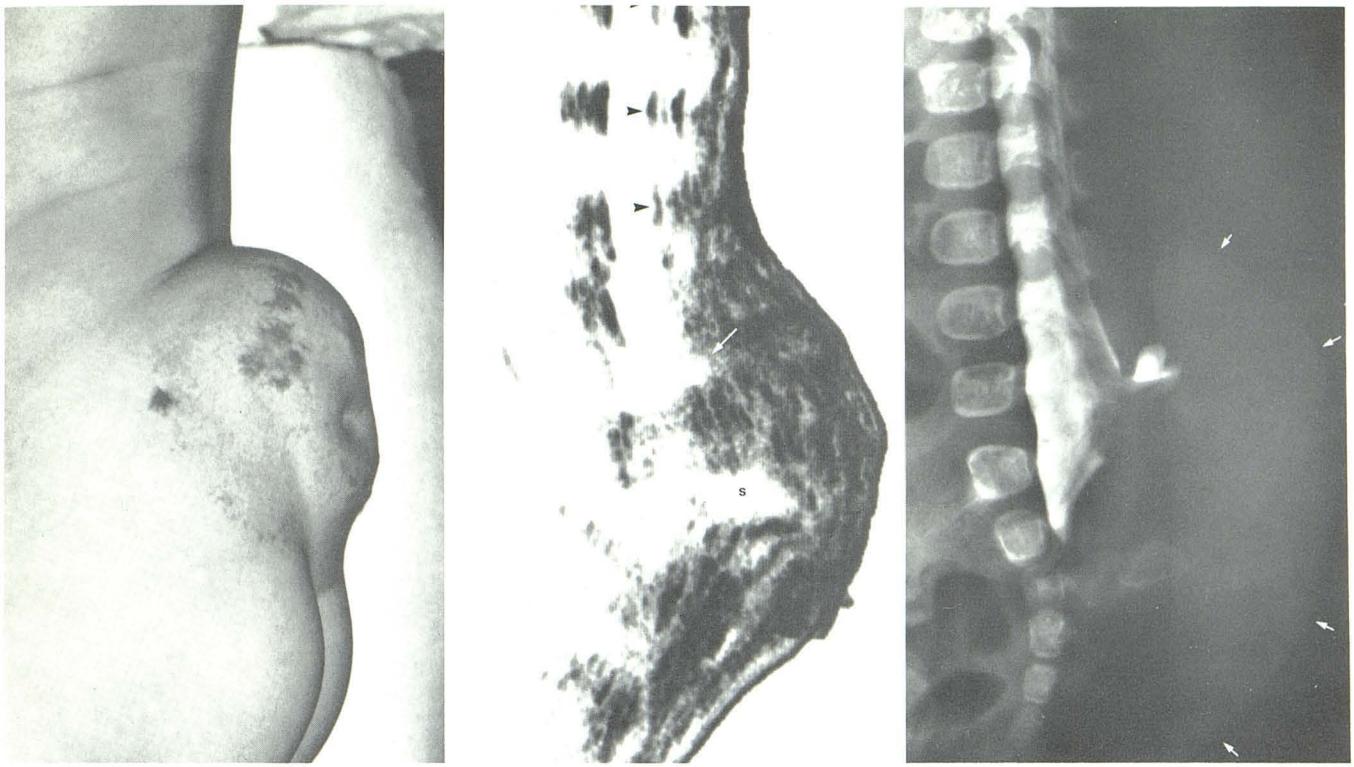

Fig. 8.—Lipomyelomeningocele with anomalous bone process, 4-month-old boy. **A**, Posterolateral view demonstrates nevus, deep skin dimple, and large lumbosacral skin-covered mass situated above intergluteal cleft. **B**, Sagittal sonogram demonstrates hyperechoic lumbosacral mass, "triplet" echoes from tethered spinal cord (*arrowheads*), posterior position of cord against inside of lumbar lordosis, widening of subarachnoid space ventral to tethered cord, and increased echogenicity where lipoma inserts onto dorsal surface of tethered cord. Small true meningocele (*arrow*) lies along upper border of mass. Acoustic shadowing (S) signifies presence of anomalous bone process or dense calcification within mass. **C**, Lateral water-soluble contrast myelogram confirms presence of lumbosacral lipoma (*arrows*), tethered cord pulled dorsally along inside of lumbar lordosis, extension of lucent lipoma into dorsal surface of cord, small superiorly situated meningocele, anomalous bone process at site of acoustic shadowing, and S3 hemicentrum. At surgery, skin dimple was connected directly to apex of bone process by fibrous band.

Sacral Agenesis and Spina Bifida

Sonography demonstrated appropriate focal absence of spinal echoes and reduced size of paraspinal and gluteal muscle mass in the two patients with complete sacral agenesis (fig. 3). Sonography displayed appropriate focal absence of inferior sacral echoes in one of the three patients with partial sacral agenesis (fig. 7), but failed to resolve the absent sacral element in each of the two patients with focal absence of one-half of the S3 centrum only (fig. 8).

Transverse sonography displayed posterior spina bifida as focal midline deficiency in the reflections from the posterior lumbodorsal fascia, wide separation of the subjacent paraspinal muscles, and abnormal orientation ("eversion") of the paraspinal muscles (figs. 4 and 5). Sagittal sonography demonstrated posterior spina bifida as appropriate focal absence of spinal echoes, provided the bony defects were of substantial size (fig. 6). However, sagittal sonography failed to identify small zones of spina bifida and failed to differentiate between true posterior spina bifida and normal but still-unossified spinal arches. For these reasons, posterior spina bifida was usually appreciated more easily on transverse than on sagittal sonograms.

Meningocele

In each of the 15 patients in whom a meningocele formed at least one component of the anomaly, sonography depicted the meningocele as an anechoic or markedly hypoechoic extracanalicular space that was directly continuous with the spinal canal through a spina bifida (figs. 6 and 7). The size and configuration of the meningocele and its relations to the spinal column, paraspinal muscles, fascial planes, and skin surface were easily appreciated in 12 of the 15 patients. In three patients with meningoceles measuring less than 5 × 5 mm, the meningocele was hard to discern without direct comparison to the myelogram. In one patient with a lipomyelomeningocele and an anomalous posterior bone process (fig. 8), the small anechoic region of the true meningocele could be differentiated from the far larger acoustic shadow produced by the anomalous bone, because increased sound transmission through the meningocele provided sharp defini-

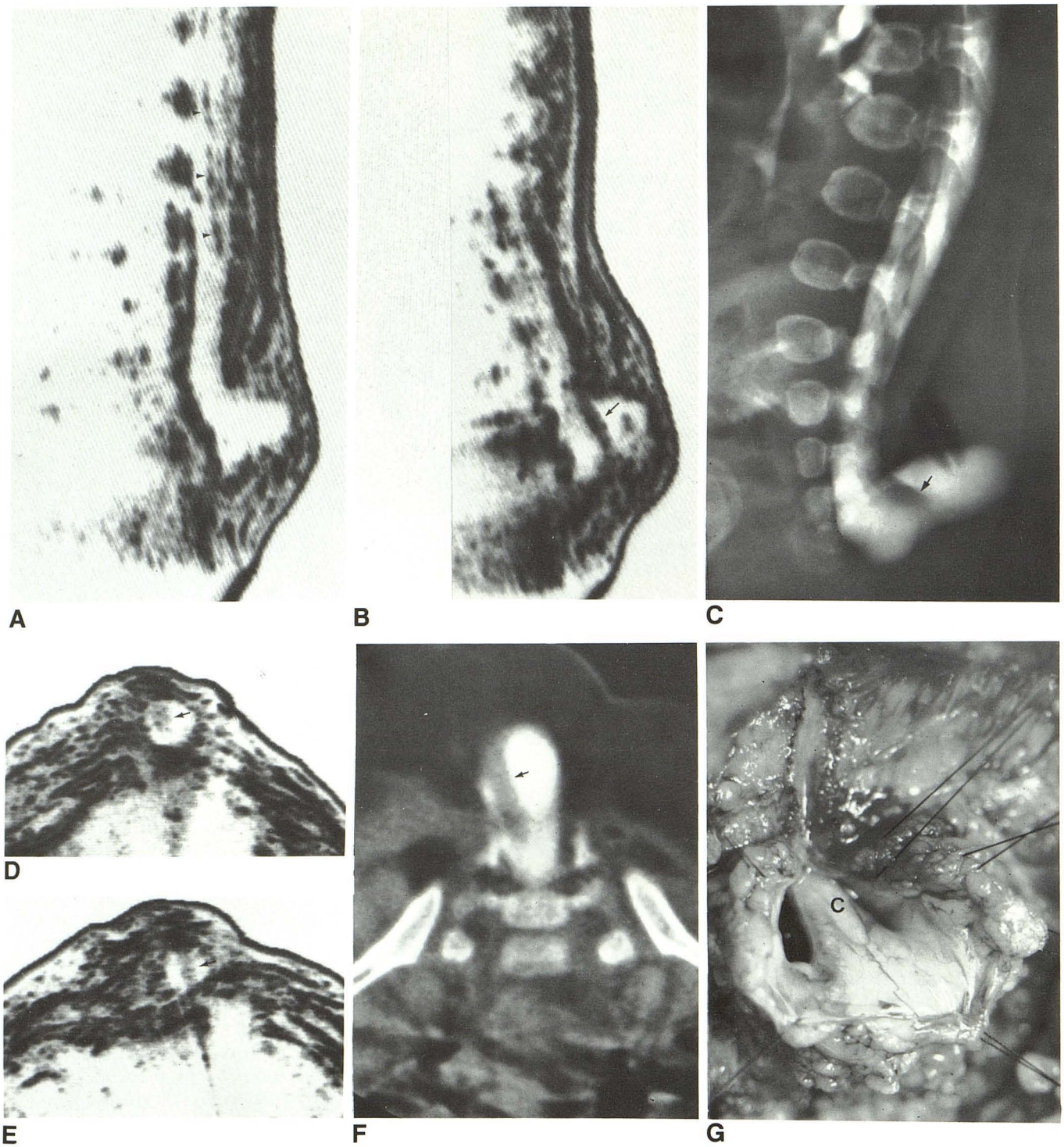

Fig. 9.—Lipomyelomeningocele with extension of filum into meningocele in 4-month-old girl with skin dimple and asymmetric skin-covered lumbosacral mass above intergluteal cleft. **A** and **B**, Sagittal sonograms reveal hyperechoic subcutaneous lumbosacral mass; large anechoic meningocele extending into mass through posterior spina bifida; "triplet" echoes from tethered spinal cord (*arrowheads*); and extension of hyperechoic structure (*arrow*) across meningocele to insert into its caudal border. **C**, Lateral water-soluble contrast myelogram confirms presence of subcutaneous lipoma, meningocele, and tethered cord. Lucent tubular structure (*arrow*) extends across meningocele from dorsal surface of distalmost cord to funnel-shaped indentation of caudal surface of sac. Transverse sonograms (**D** and **E**) and axial water-soluble contrast CT myelogram (**F**) demonstrate hyperechoic lucent lipoma, anechoic meningocele, and tubular structure (*arrows*) that traverses meningocele to insert at its dome. **G**, Posterolateral operative photograph after opening meningocele from behind demonstrates large surrounding lipoma, tethered cord (C), and markedly thickened filum terminale. (**G** is courtesy of Francisco Gutierrez, Chicago.)

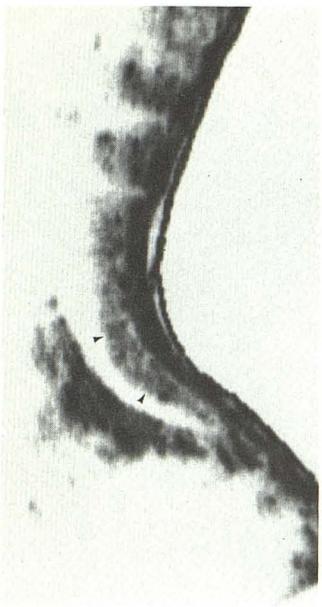

Fig. 10.—Postoperative myelomeningocele with retethering of spinal cord in 8-year-old boy. Findings confirmed by myelography and surgery. Midsagittal sonogram demonstrates increased lumbar lordosis; lumbar spina bifida with absence of posterior spinal echoes; and thickened, hyperechoic scar tissue over spina bifida. Tethered spinal cord (*arrowheads*) is hyperechoic, pulled posteriorly along inside of lordotic curve, and inseparable from hyperechoic scar caudally. Ventral subarachnoid space is widened. At surgery, open placode of tethered cord was densely adherent to dorsal dural closure.

tion of the subjacent canal wall, whereas the reduced transmission through the bone process prevented delineation of the subjacent canal wall.

Spinal Cord and Nerve Roots

Sonography documented normal cord position in each of the 10 patients in whom this was the true state, including one patient with a lipoma and cord fixation at a higher level and a second patient with lipoma of the filum terminale. Sonography demonstrated low position of the intracanalicular part of the spinal cord in 16 (94%) of the 17 patients with low cord position (fig. 8), but failed to visualize the spinal cord adequately in one patient with lipomyelomeningocele and tethered cord. Sonography correctly displayed extracanalicular extension of the spinal cord or filum terminale into a meningocele in seven of 10 patients (fig. 9), and did not falsely suggest such extension in any patient.

The sonographic appearance of the low-lying cord varied in the 16 patients. In eight patients of diverse ages, sagittal sonography demonstrated the low-lying cord as "triplet" echoes representing the anterior surface, posterior surface, and central canal of the spinal cord (figs. 8 and 9). In three other patients, including one of the three with hydromyelia, only the anterior and posterior surfaces of the cord could be visualized. In two patients, the low-lying spinal cord was so tightly applied to the posterior wall of the spinal canal that only the echoes from the anterior surface of the cord could be resolved. In the two patients with retethering of a previously repaired myelomeningocele, the low-lying cord appeared solid and echogenic (fig. 10). In one patient, the cord echoes were poorly resolved and difficult to categorize. The descending nerve roots of the cauda equina were resolved in eight cases, and closely resembled the anterior and posterior surfaces of a low-lying spinal cord in two cases (fig. 2).

Lipoma

Sonography successfully displayed the presence, site, size, and configuration of the subcutaneous and/or intraspinal lipoma in 14 of 15 patients. In the 15th patient (fig. 11), a 1 × 2 cm intra- and extracanalicular lipoma that inserted onto the dorsal surface of the spinal cord at L1–L3 could not be appreciated on the sonogram, even in retrospect. There was no associated meningocele. Sonography demonstrated both *lipomas of the filum terminale* as abnormally thick, hyperechoic curvilinear structures that conformed to the course of the filum. Sonography demonstrated each *lipomyelomeningocele* as a highly echoic, slightly lobulated, subcutaneous mass that formed the border of an anechoic meningocele and inserted onto the surface of the spinal cord (figs. 8 and 9). When the spinal cord protruded through the spina bifida into the subcutaneous space, the conjunction of cord and lipoma typically lay outside the spinal canal. The intracanalicular part of the spinal cord typically was pulled dorsally against the posterior wall of the spinal canal and the ventral subarachnoid space was consequently widened (fig. 8). When the spinal cord remained within the spinal canal, the lipoma typically extended into the spinal canal, and the conjunction of cord and lipoma lay within the spinal canal. The spinal cord was then typically displaced anteriorly by the intracanalicular component of the lipoma, and the subarachnoid space was widened behind the cord and above the intracanalicular lipoma (fig. 12). In eight cases, the distal spinal cord exhibited increased echogenicity along its junction with lipoma suggesting cephalic extension of lipoma along the dorsal myeloschisis and within the central canal of cord [20, 21].

The lipoma was substantially more echogenic than the subcutaneous fat or the neural tissue in each of the 14 lipomas depicted successfully. The solid, fibroadipose parts of the two teratomas in this series were also substantially more echogenic than either subcutaneous fat or neural tissue. Thus far, we have not appreciated any *hypo*echoic lipoma [9], but must consider the possibility that the lipoma we failed to detect may have been such a case.

Sacrococcygeal Teratoma

Sonography depicted both teratomas successfully. One of the two teratomas appeared homogeneously echogenic and indistinguishable from solid lipoma. This mass proved to be a benign teratoma composed predominantly (70%) of fibroadipose tissue. Multiple cystic spaces, the largest of which measured 1.1 × 0.5 × 0.4 cm, were not appreciated sonographically. The second teratoma exhibited both a small superficial hyperechoic fibroadipose component and a large, deep, anechoic, bicystic component that extended into the pelvis anterior to a normally formed sacrum and coccyx (fig. 13). Neither teratoma entered the spinal canal.

Wholly Intracanalicular Mass

Sonography successfully demonstrated the single wholly intracanalicular mass in our series. This intramedullary der-

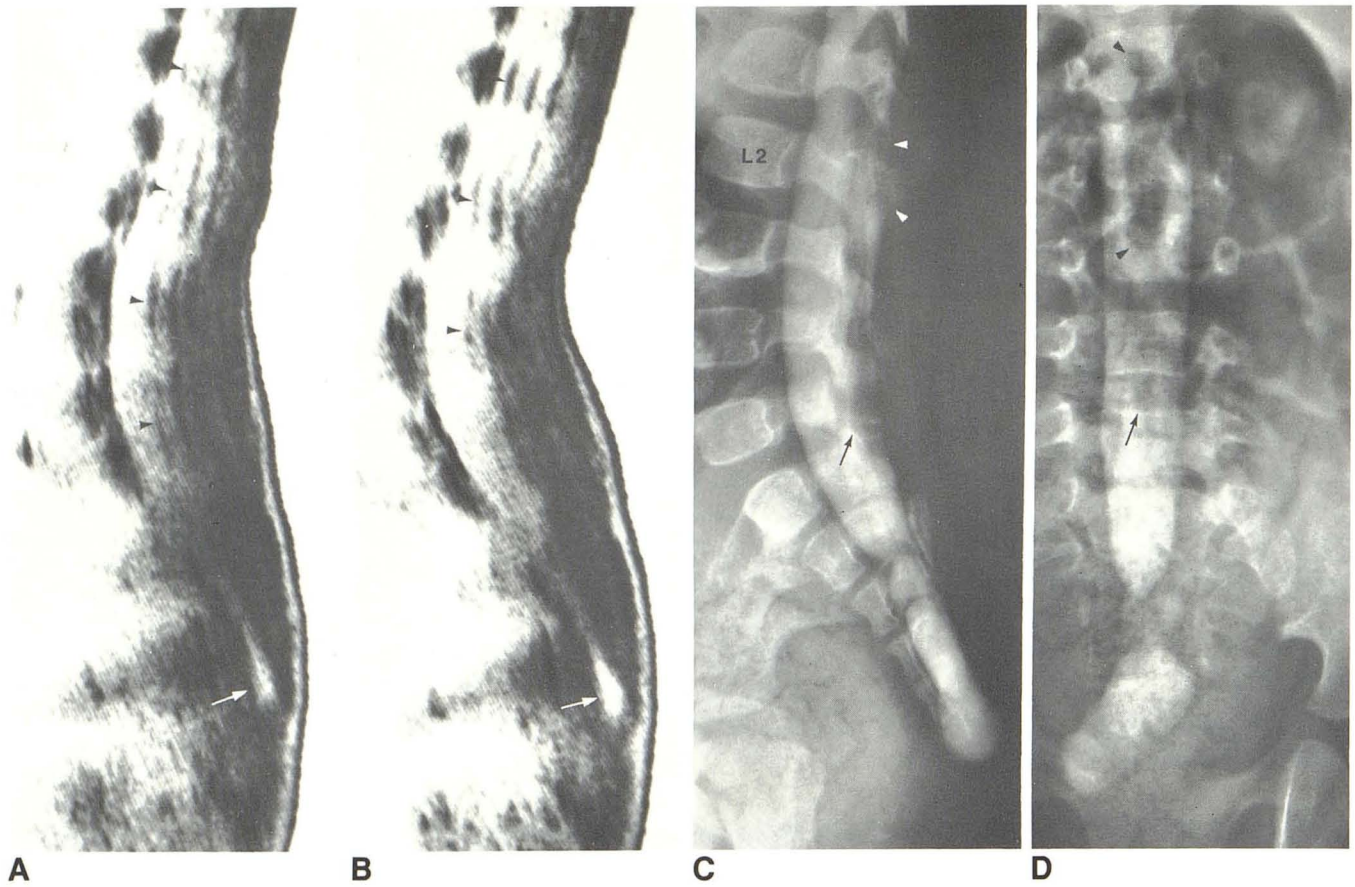

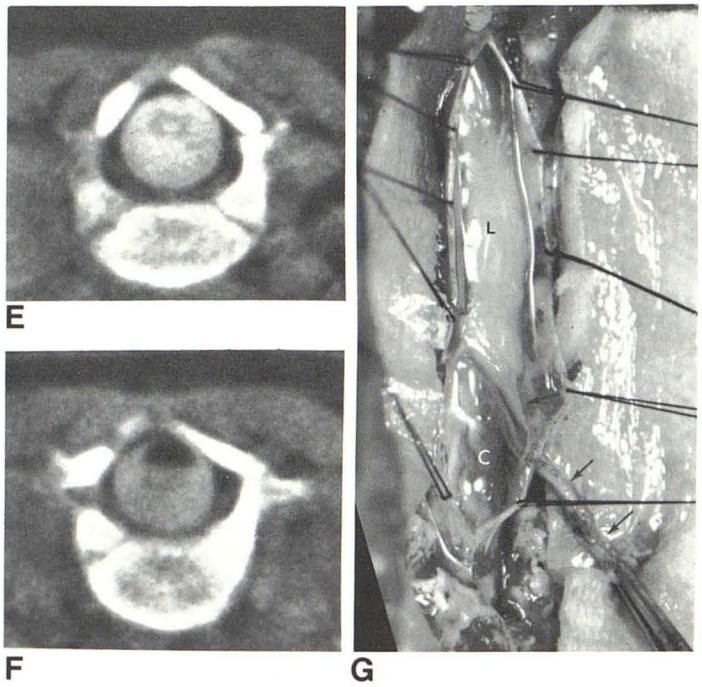

Fig. 11.—Spinal lipoma with distant simple meningocele, 11-month-old girl. **A** and **B**, Sagittal sonograms demonstrate "triplet" echoes from tethered spinal cord (*arrowheads*), displacement of cord to inside of lordosis, widened anechoic ventral subarachnoid space, and anechoic terminal meningocele (*arrows*). No hyperechoic intracanalicular lipoma can be discerned. Water-soluble contrast myelography in lateral (**C**) and posteroanterior (**D**) projections demonstrates asymmetric terminal simple meningocele and lucent mass (*arrowheads*) dorsal to cord at L2, well above tip (*arrows*) of low-lying cord. Axial water-soluble contrast CT myelographic sections above level of mass (**E**) and at mass (**F**) reveal small, posteriorly positioned cord with dilated, opacified central canal and lipoma dorsal to cord at L2. **G**, Posterolateral view of surgical field demonstrates lipoma (L) dorsal to cord (C); extension of cord well caudad from lipoma; and fibrous stalk (*arrows*) (cut end held by forceps), which passes from extradural space through dura (held open by sutures) into lower pole of lipoma. Fibrous stalk contained no epithelial elements.

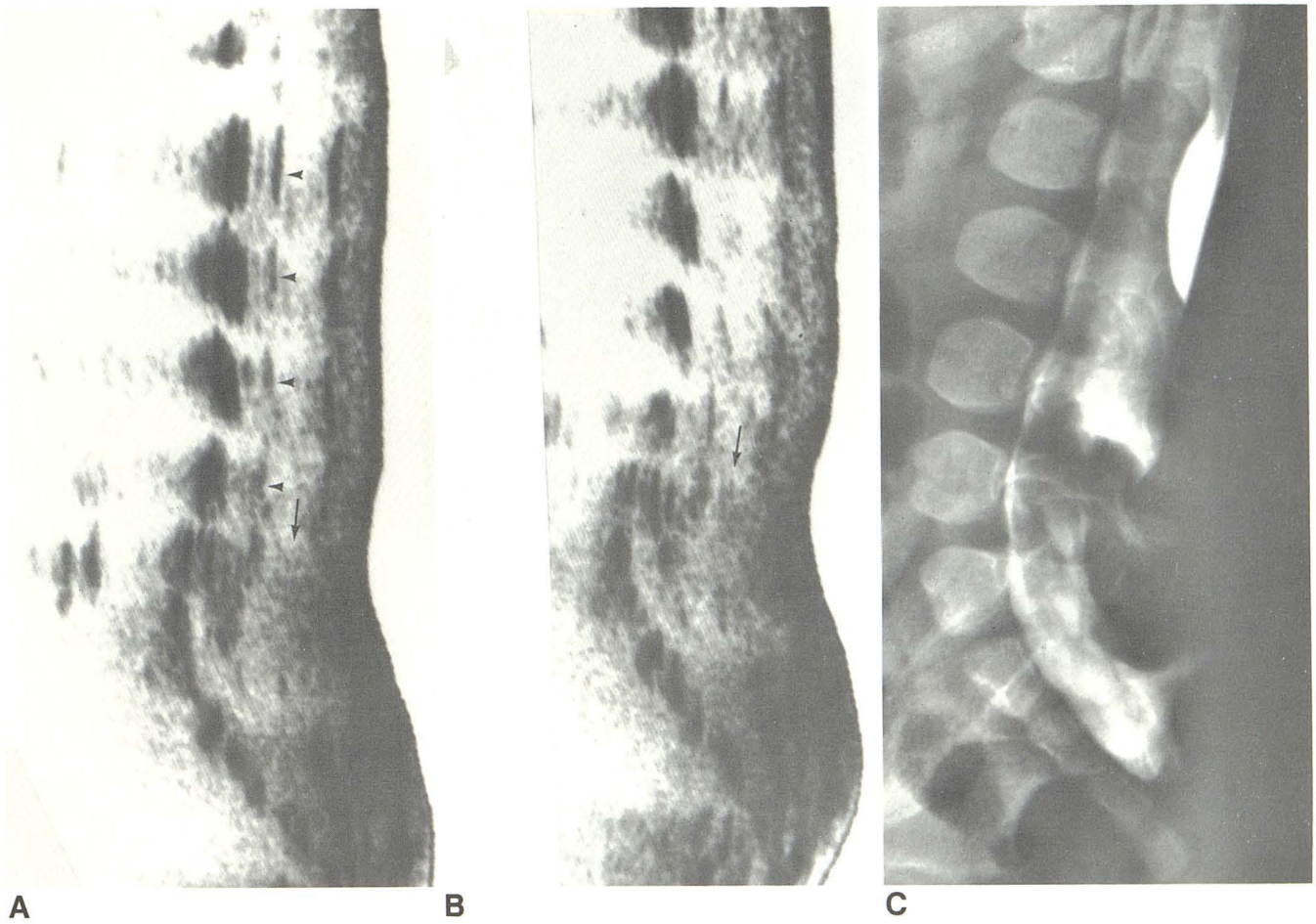

Fig. 12.—Lipomyelomeningocele with anterior displacement of tethered cord in 10-month-old boy. **A** and **B**, Midsagittal sonograms demonstrate hyperechoic skin-covered lipoma, posterior spina bifida, tethered spinal cord (*arrowheads*) displaced anteriorly by extension of hyperechoic mass (*arrows*) into canal, and increased echogenicity of distal cord, possibly representing insertion of lipoma onto dorsal surface of cord. Thickened filum terminale was shown on other sections. **C**, Lateral water-soluble contrast myelogram confirms anterior displacement of tethered spinal cord by hyperlucent mass, which is continuous with subcutaneous lipoma through posterior lumbosacral spina bifida. Filum terminale is thickened.

moid appeared as a round, nearly homogeneous, mildly echogenic mass situated eccentrically within the sacral spinal canal (fig. 6).

Discussion

We chose to use articulated-arm B-mode sonography for this study rather than real-time B-mode sonography because the articulated-arm images display a far greater length of spinal column and cord in a single image. This longer anatomic section permits ready, confident identification of the vertebral levels depicted, the position of the normal or tethered spinal cord, and the complex interrelations of spinal, neural, and tumoral components of the lesions. In our opinion, real-time sonography of the distal cord to evaluate damping of cord pulsation by tethering mass [9] is a useful but supplemental examination.

Interpretation

The normal position of the conus medullaris was reviewed by Barson [22]. In adults and older children, the conus medullaris normally lies along the posterior surface of the spinal canal at L1–L2. In infants less than 3 months of age, the tip of the conus may normally lie more caudally at L2–L3, rarely lower. In practical terms, a spinal cord that is imaged below this level is best regarded as abnormally low in position and possibly tethered.

The spinal cord normally follows the inside of any spinal curvature. In patients with spinal dysraphism, the normal spinal curvatures are often exaggerated and there are additional (kypho)scolioses. The spinal cord is then even more tightly applied to the inner (concave) surface of each of the continually changing curves, leaving wide subarachnoid spaces along the outer surface of each curve. A spinal cord may fail to follow the inside of the curve for one of two

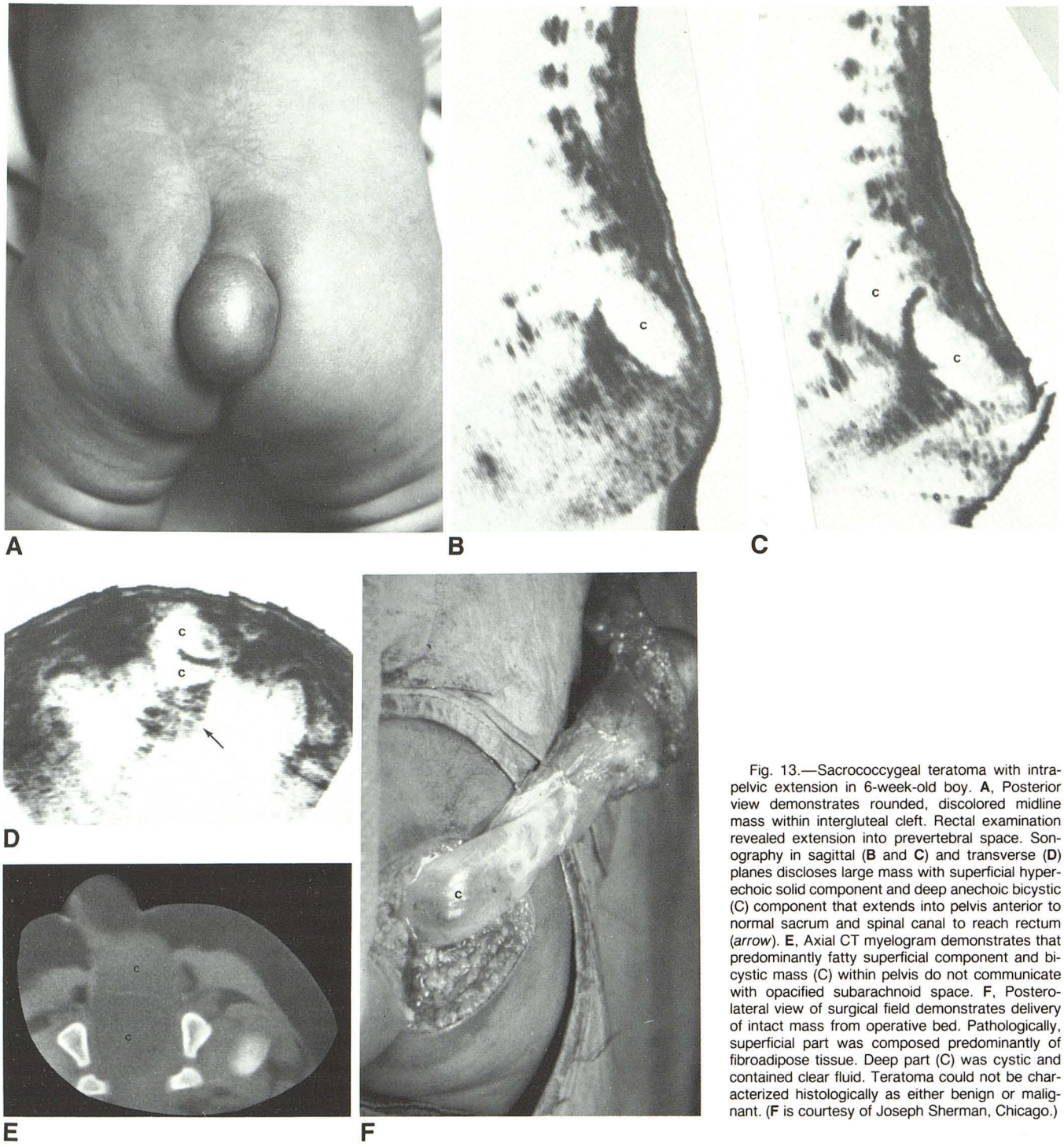

Fig. 13.—Sacrococcygeal teratoma with intrapelvic extension in 6-week-old boy. **A**, Posterior view demonstrates rounded, discolored midline mass within intergluteal cleft. Rectal examination revealed extension into prevertebral space. Sonography in sagittal (**B** and **C**) and transverse (**D**) planes discloses large mass with superficial hyperechoic solid component and deep anechoic bicystic (C) component that extends into pelvis anterior to normal sacrum and spinal canal to reach rectum (*arrow*). **E**, Axial CT myelogram demonstrates that predominantly fatty superficial component and bicystic mass (C) within pelvis do not communicate with opacified subarachnoid space. **F**, Posterolateral view of surgical field demonstrates delivery of intact mass from operative bed. Pathologically, superficial part was composed predominantly of fibroadipose tissue. Deep part (C) was cystic and contained clear fluid. Teratoma could not be characterized histologically as either benign or malignant. (**F** is courtesy of Joseph Sherman, Chicago.)

reasons: (1) it is tethered and stretched tightly ("bow-strung") across several levels of curvature or (2) it is displaced away from the inside of the curve by an intracanalicular component of mass.

Tethered spinal cords often appear thinner than normal. Such narrow caliber could conceivably represent cord stretching. In patients with myelodysplasia, however, the "reduced" weight of each segment of the "thin" cord may be in proper proportion to the reduced body weight of the patient [23].

The reason the two myelodysplastic cords appeared homogeneously hyperechoic is unknown. According to Emery and Lendon [24], fibrolipomas are found in the dura adjacent to the neural placode in 7% of myelomeningocele patients. More complex forms of lipoma, *leptomyelolipomas*, are found

near the conus medullaris in another 7% of myelomeningocele patients. Postsurgical implantation lipomas occur in the subarachnoid space and diverse layers of the surgical closure in another 5% of cases. Concurrent lipoma could then contribute to the increased echo density observed in these tethered cords. Scarring related to prior infection or prior surgery may also have played a role.

We believe that part of the echogenicity of lipomas derives from the fibrous septa that divide the lipoma into fine lobules and provide multiple reflective interfaces. However, Behan and Kazam [25] have shown that, even in the absence of fibrous tissue, fat may be *hyper*echoic, or *hypo*echoic, depending on the relative proportions and degree of dispersion of its lipid and aqueous constituents.

Unresolved Diagnostic and Technical Problems

A number of unresolved problems limit our understanding of spinal sonography, limit its usefulness for patient screening, and mandate great care in analyzing the images obtained and circumspection in applying the results to patient management:

Hyperechoic versus anechoic vertebral bodies. We do not understand why vertebral elements seem to appear hyperechoic on sagittal sonograms but hypoechoic or anechoic in transverse sonograms. We believe this phenomenon is related to differing angles of incidence and reflectance of the sonic beam or to other technical factors. However, we cannot exclude the possibility that we have misinterpreted the observations on sagittal sonograms and are reading echoes from juxtaosseous soft tissue as hyperechoic vertebral bodies. Such error would seriously diminish our understanding of the sonographic images but would not affect the validity of the criteria used for diagnosing the presence and nature of caudal spinal anomalies.

Cauda equina versus tethered cord. The echoes from the spinal cord, particularly the low-lying cord, usually curve posteriorly along the inside of the lumbar lordosis. The echoes from the roots of the cauda equina usually incline anteroinferiorly toward the ventrally situated root sleeves and are appreciably less intense, more crowded, and more undulant than those from the spinal cord. However, in some patients, the anterior nerve roots of the cauda equina descend in one coronal plane while the posterior roots descend in a second coronal plane behind the first. The echoes from the two sets of roots may then mimic the anterior and posterior surfaces of a tethered cord on sagittal sonograms and cause diagnostic confusion (fig. 3). Conversely, in those patients with an intracanalicular mass that tethers the cord, displaces it anteriorly, and damps its pulsation [8], the unusual anterior course and reduced intensity of echoes from the cord could cause it to be mistaken for the descending roots of the cauda equina (fig. 12). In patients with hydromyelia involving the low-lying segment of the cord, the echoes from widely separated anterior and posterior surfaces of cord could also be mistaken for the cauda equina.

Bone processes and calcification versus meningocele. It would appear likely that acoustic shadows from anomalous bone processes or from dense calcifications within a subcutaneous mass could be misinterpreted as anechoic meningoceles if the degree of sound transmission deep to the "lesion" were not analyzed carefully and/or if the sonograms were not compared with plain spine radiographs (fig. 8).

Lipoma versus teratoma. It would also appear likely that the similar sonographic appearances of lipoma and solid teratoma and of lipomyelomeningocele and cystic teratoma could lead to misdiagnosis. Indeed, in our series, the sacral lesion signed out pathologically as "malformative process, cannot rule out teratoma" included a small cyst immediately superficial to a spina bifida and closely resembled a complex form of meningocele without cord tethering. The risk of such misdiagnosis is reduced if it is remembered that, clinically, nearly all spinal lipomas form soft-tissue masses that lie above the intergluteal cleft (even if they extend asymmetrically into one buttock). Conversely, most teratomas form masses within or below the intergluteal cleft (fig. 13). Further, most lumbosacral lipomas pass deeply through a spina bifida into the spinal canal, whereas most of the teratomas that extend deeply pass beneath the normal sacrum into the pelvis without entering the spinal canal.

Dorsal sinus versus pilonidal sinus. In this small series of patients, it has not been possible to examine a dermal sinus to see whether sonography can demonstrate extension of a dermal sinus to the bone surface or into the spinal canal. Therefore, although the pilonidal sinuses have all exhibited similar features, we cannot know whether sonography can distinguish pilonidal from dermal sinus.

Excluded patient populations. Sonography is difficult to perform safely or effectively in some specific groups of patients. Newborns with exposed, friable myelomeningoceles cannot be studied by direct contact scanning lest the procedure traumatize the exposed neural tissue and introduce infection. This group could be studied with a water-bath technique. Direct contact scanning cannot be used in the immediate postoperative period because edema and hemorrhage distort the tissue planes and because bandages prevent good acoustic coupling. Older myelomeningocele children with dense midline scars at the site of surgical repair often cannot be studied adequately by direct contact scanning because the sonographic beam penetrates the scar too poorly to depict the subjacent cord and canal. These important groups of patients are therefore excluded from the screening procedure.

Despite these difficulties, sonography remains an inexpensive, noninvasive examination easily applied to clinic populations with possible spinal anomalies. At Children's Memorial Hospital, Chicago, sonography has already proved useful for confirming clinical impressions of tethered spinal cord, simple meningocele, lipomyelomeningocele, sacrococcygeal teratoma, and pilonidal sinus. Sonography has assisted us in convincing parents and referring physicians to expedite admitting these patients to the hospital for definitive examination and for any surgery necessary. However, until far greater experience permits us to determine the precise sensitivity and accuracy of sonographic diagnosis, we consider it inadvisable to use sonography as the sole screening method and

routinely refer clinically suspicious but "sononegative" patients for standard radiographic evaluation.

ACKNOWLEDGMENTS

We thank Andrew K. Poznanski for helpful suggestions; Carol Fabian for manuscript assistance; Suzanne Devine and Maria Manolovic for sonographic assistance; Carol Freda, Patricia Garland, Olga Guzman, Arthur Nieves, Ernesto Salazar, Jr., and Gloria Short for assistance in CT preparation; and David Weil and Kascot Media, Inc., for photographic assistance.

REFERENCES

1. Babcock DS, Han BK. Cranial sonographic findings in meningomyelocele. *AJNR* **1980**;1:493–499, *AJR* **1981**;136:563–567
2. Shkolnik A, McLone DG. Intraoperative real-time ultrasound guidance of ventricular shunt placement in infancy. *Radiology* **1971**;141:515–517
3. Slovis TL, Kuhns LR. Real-time sonography of the brain through the anterior fontanelle. *AJR* **1981**;136:277–286
4. Chopra A, Teele RL. Hydronephrosis in children: narrowing the differential diagnosis with ultrasound. *JCU* **1980**;8:473–478
5. Boal DKB, Teele RL. Sonography of infantile polycystic kidney disease. *AJR* **1980**;135:575–580
6. Williams PL, Warwick R, eds. *Gray's anatomy*, 36th ed. Philadelphia: Saunders, **1980**:282–283
7. Leopold GR. Ultrasonography of superficially located structures. *Radiol Clin North Am* **1980**;18:161–173
8. Miller JH, Reid BS, Kemberling CR. Utilization of ultrasound in the evaluation of spinal dysraphism in children. *Radiology* **1982**;143:737–740
9. Scheible W, James HE, Leopold GR, Hilton SW. Occult dysraphism in infants: screening with high-resolution real-time ultrasound. *Radiology* **1983**;146:743–746
10. Naidich TP, McLone DG, Shkolnik A, Fernbach SK. Sonographic evaluation of caudal spine anomalies in children. *AJNR* **1983**;4:661–664
11. Hibbert CS, Delaygue C, McGlen B, Porter RW. Measurement of the lumbar spinal canal by diagnostic ultrasound. *Br J Radiol* **1981**;54:905–907
12. Kadziolka R, Asztely M, Hanai K, Hansson T, Nachemson A. Ultrasonic measurement of the lumbar spinal canal. The origin and precision of the recorded echoes. *J Bone Joint Surg [Br]* **1981**;63:504–507
13. Finlay D, Stockdale HR, Lewin E. An appraisal of the use of diagnostic ultrasound to quantify the lumbar spinal canal. *Br J Radiol* **1981**;54:870–874
14. Rubin JM, Dohrmann GJ. Work in progress: intraoperative ultrasonography of the spine. *Radiology* **1983**;146:173–175
15. Braun IF, Raghavendra BN, Kricheff II. Spinal cord imaging using real-time high-resolution ultrasound. *Radiology* **1983**;147:459–465
16. Reid MH. Ultrasonic visualization of a cervical cord cystic astrocytoma. *AJR* **1978**;131:907–908
17. James HE, Scheible W, Kerber C, Hilton SvW. Comparison of high resolution real time ultrasonography and high resolution computed tomography in an infant with spinal dysraphism. *Neurosurgery* **1983**;13:301–305
18. Shkolnik A. Gray scale ultrasound of the pediatric abdomen and pelvis. *Curr Probl Diagn Radiol* **1977**;7:1–41
19. McCreath GT, Macpherson P. Sonography in the diagnosis and management of anterior sacral meningocele. *JCU* **1980**;8:133–137
20. Naidich TP, McLone DG, Harwood-Nash DC. Dysraphism. In: Newton TH, Potts DG, eds. *Modern neuroradiology*, vol 1. *Computed tomography of the spine and spinal cord*. San Francisco: Clavadel, **1983**:299–353
21. Naidich TP, McLone DG, Mutluer S. A new understanding of dorsal dysraphism with lipoma (lipomyeloschisis): radiologic evaluation and surgical correction. *AJNR* **1983**;4:103–116, *AJR* **1983**;140:1065–1078
22. Barson AJ. The vertebral level of termination of the spinal cord during normal and abnormal development. *J Anat* **1970**;106:489–497
23. Barson AJ, Sands J. Physical and biochemical characteristics of the human dysraphic spinal cord. *Dev Med Child Neurol* **1975**;17[Suppl 35]:11–19
24. Emery JL, Lendon RG. Lipomas of the cauda equina and other fatty tumors related to neurospinal dysraphism. *Dev Med Child Neurol* **1969**;11[Suppl 20]:62–70
25. Behan M, Kazam E. The echocardiographic characteristics of fatty tissues and tumors. *Radiology* **1978**;129:143–151